# Solution Structure of α-Conotoxin ImI by $^1$H Nuclear Magnetic Resonance†

John Gehrmann, Norelle L. Daly, Paul F. Alewood, and David J. Craik*

*Centre for Drug Design and Development, University of Queensland, Brisbane, Queensland 4072, Australia*

*Received March 12, 1999*

α-Conotoxin ImI derives from the venom of *Conus imperialis* and is the first and only small-peptide ligand that selectively binds to the neuronal $\alpha_7$ homopentameric subtype of the nicotinic acetylcholine receptor (nAChR). This receptor subtype is a possible drug target for several neurological disorders. The cysteines are connected in the pairs Cys2−Cys8 and Cys3−Cys12. To date it is the only α-conotoxin with a 4/3 residue spacing between the cysteines. The structure of ImI has been determined by $^1$H NMR spectroscopy in aqueous solution. The NMR structure is of high quality, with a backbone pairwise rmsd of 0.34 Å for a family of 19 structures, and comprises primarily a series of nested $\beta$ turns. Addition of organic solvent does not perturb the solution structure. The first eight residues of ImI are identical to the larger, but related, conotoxin EpI and adopt a similar structure, despite a truncated second loop. Residues important for binding of ImI to the $\alpha_7$ nAChR are all clustered on one face of the molecule. Once further binding data for EpI and ImI are available, the ImI structure will allow for design of novel $\alpha_7$ nAChR-specific agonists and antagonists with a wide range of potential pharmaceutical applications.

## Introduction

*Conus* spp. are a group of hunting marine snails that paralyze their prey (worms, mollusks, or fish) by injecting a venom which consists of a cocktail of peptide toxins.[1,2] These conotoxins are predominantly disulfide-rich peptides that selectively target specific receptors and ion channels critical to the functioning of the neuromuscular system. Conotoxins are short compared with other polypeptide toxins, varying in length from approximately 10 to 30 residues.

The α-conotoxin family is characterized by two conserved disulfide bonds which link the first and third and the second and fourth cysteine residues (i.e. 1−3, 2−4 connectivity), nominally forming two loops in the peptide backbone between cysteine residues (Figure 1). The number of amino acids between these disulfide bonds varies between different family members, from three to four in the first loop and from three to seven in the second. All members of the α-conotoxin family inhibit nicotinic acetylcholine receptors (nAChRs) in muscle, neurons, or both.

α-Conotoxin ImI, isolated from the worm-hunting *Conus imperialis*,[3] is unusual in that even though its first eight residues are identical to the corresponding sequence from EpI,[4] a recently discovered α-conotoxin from *C. episcopatus*, the second loop only contains three residues compared with seven in EpI. Indeed, the 4/3 loop spacing of ImI is different from all of the other known neuronal nAChR blockers, which have a 4/7 loop spacing as indicated in Figure 1.[5,6] By contrast most muscle-specific α-conotoxins have a 3/5 spacing.[7]

The nAChR is part of the ligand-gated ion channel (LGIC) superfamily, which includes the $GABA_A$, serotonin, and GluCl glutamate receptors.[8] All of the LGICs are large, membrane-bound pentamers with various subunit compositions and several conserved features. Each subunit is postulated to contain four transmembrane helices (M1 to M4), with the M2 helix lining the selective ion channel lumen. Binding of an endogenous ligand to a large, extracellular domain remote to the M2 helix brings about a conformational change in the M2 helices that causes the pore to open. The acetylcholine receptor is intimately involved in transduction of signals in the brain and at the neuromuscular junction.[9−11] Of the two subclasses of nAChR (muscular and neuronal), the muscle type nAChR is a heteropentamer composed of two $\alpha_1$ subunits and one each of $\beta_1$, $\gamma$, and $\delta$ or $\epsilon$ subunits. The neuronal nAChRs are either heteropentamers made up of $\alpha_{(2-6)}$ and $\beta_{(2-4)}$ subunits or homopentamers composed of $\alpha_7$ or $\alpha_9$ subunits.

Even though the neuronal nAChRs play a key role in the central and peripheral nervous system, their study is hampered by the complexity of their subtype association, function, and distribution. Often mixtures of receptors are colocalized in various brain regions, and hence physiological study is made difficult, as very specific probes are required to distinguish these receptors. ImI is the only small peptide specific to the homopentameric neuronal nAChRs composed of $\alpha_7$ and, to a lesser extent, $\alpha_9$ subunits.[12] This makes it a very important neurological tool.

The precise physiological role of the $\alpha_7$ homomer is not as yet fully understood, although it has been shown to possess a $Ca^{2+}$-specific pore, compared to the normal

* To whom correspondence should be addressed. Tel: 617 3365 4945. Fax: 617 3365 2487. E-mail: D.Craik@mailbox.uq.edu.au.

† Abbreviations: 1D, one-dimensional; 2D, two-dimensional; 3D, three-dimensional; ACN, acetonitrile; Boc, *tert*-butoxycarbonyl; DMF, *N*,*N*-dimethylformamide; DQF-COSY, 2D double-quantum-filtered *J*-correlated spectroscopy; DSS, 4,4-dimethyl-4-silapentane-1-sulfonate; ECOSY, 2D exclusive *J*-correlated spectroscopy; HMQC, 2D heteronuclear multiple-quantum coherence spectroscopy; HPLC, high-performance liquid chromatography; LGIC, ligand-gated ion channel; MBHA, 4-methylbenzhydrylamine; nAChR, nicotinic acetylcholine receptor; NOE, nuclear Overhauser effect; NOESY, 2D NOE spectroscopy; ppb, parts per billion; ppm, parts per million; rmsd, root-mean-square deviation; TFA, trifluoroacetic acid; TFE, trifluoroethanol; TOCSY, 2D total correlated spectroscopy.

10.1021/jm990114p CCC: $18.00 
Published on Web 06/11/1999

| Name: | Sequence: | Receptor Target: | Species: | Prey: |
|---|---|---|---|---|
| ImI | GCCSDPRCAWR----C-$NH_2$ | n ($\alpha_7$) | *C. imperialis* | Worms |
| EpI | GCCSDPRCNMNNPDYC-$NH_2$ | n ($\alpha_3\beta_2$, $\alpha_3\beta_4$) | *C. episcopatus* | Molluscs |
| PnIA | GCCSLPPCAANNPDYC-$NH_2$ | n | *C. pennaceus* | Molluscs |
| PnIB | GCCSLPPCALSNPDYC-$NH_2$ | n | *C. pennaceus* | Molluscs |
| MII | GCCSNPVCHLEHSNLC-$NH_2$ | n ($\alpha_3\beta_2$) | *C. magus* | Fish |
| EI | RDOCCYHPTCNMSNPQIC-$NH_2$ | m ($2\alpha_1\beta\gamma(\delta/\varepsilon)$) | *C. ermineus* | Fish |
| GI | ECC-NPACGRHYS--C-$NH_2$ | m ($2\alpha_1\beta\gamma(\delta/\varepsilon)$) | *C. geographus* | Fish |
| MI | GRCC-HPACGKNYS--C-$NH_2$ | m ($2\alpha_1\beta\gamma(\delta/\varepsilon)$) | *C. magus* | Fish |
| SI | ICC-NPACGPKYS--C-$NH_2$ | m ($2\alpha_1\beta\gamma(\delta/\varepsilon)$) | *C. striatus* | Fish |
| SII | GCCC-NPACGPNYG--CTSCS-OH | m ($2\alpha_1\beta\gamma(\delta/\varepsilon)$) | *C. striatus* | Fish |

**Figure 1.** α-Conotoxin family. Sequences are aligned using the conserved cysteine framework, boxed in gray. All toxins have an amidated C-terminus, except for SII, which is in the free acid form. SII also has an extra disulfide bond joining the two cysteine residues not involved in the normal disulfide framework. Sources: ImI,[3] EpI,[4] PnIA and PnIB,[5] MII,[6] EI,[54] GI,[55] MI,[56] SI,[57] SII;[58] n, neuronal; m, neuromuscular junction.

monovalent cation channels formed by the muscle type nAChRs. As attenuation of $Ca^{2+}$ levels is one mechanism of regulating early gene expression, the $\alpha_7$ nAChR has been postulated to be involved in early neuronal development.[13] There have only been a few cases where it has been shown that the $\alpha_7$ nAChR is actively involved in nerve signal transmission, despite the high expression of $\alpha_7$ subunits in many areas of the brain, especially the hippocampus. It appears that its major role may involve modulating other currents, enhancing fast excitatory transmissions by increasing presynaptic $Ca^{2+}$ concentrations, which in turn activates glutamatergic and cholinergic synaptic transmission.[11] The changes in sensory processing in schizophrenia have been linked to mutations in the $\alpha_7$ subunit.[14] Changes in neurite outgrowth in the hippocampus upon intraventricular administration of α-bungarotoxin, which binds $\alpha_7$ subunits with high affinity, have also indicated a role for $\alpha_7$ nAChRs in neuronal growth and plasticity.[13,15]

The $\alpha_7$ homomeric nAChR has emerged as a very important target in several disease states. The potential therapeutic value of a highly specific agonist is evident from findings that high doses of nicotine are beneficial to sufferers from cognitive and attention deficits, Parkinson's disease, Tourette's syndrome, and ulcerative colitis, as well as schizophrenia. However the side effects, including those on cardiovascular and gastrointestinal systems, dependence, sleep disturbance, and seizures, arising from high nicotine doses can be more detrimental than the main curative function,[16] and alternative ligands are of much interest, as is an understanding of the receptor structure.

Due to the large size of nAChRs (~250 kDa) the only structural information reported to date has been of low resolution (~7.5−9 Å) based on electron microscopy studies.[17,18] The receptors are approximately 65 Å in diameter, with a 25 Å depression in the middle, and are approximately 110 Å long perpendicular to the membrane bilayer. To better understand the structure and function of these receptors, it is necessary to get higher resolution data. One method for obtaining this is by studying the structures of the ligands to these receptors.

The structures of several α-conotoxins have been determined, including solution studies on GI,[19,20] MI,[21] and MII[22,23] and X-ray crystallographic studies of GI,[24] PnIA,[25] PnIB,[26] and EpI.[27] In general the neuronal-specific blockers have similar structures which consist of a central α helix over residues 6−12 and $\beta$ turns, or single turns of helix, at the N- and C-termini. Because of its unique spacing of intracystine loops and its selectivity for the $\alpha_7$ nAChR, it was of interest to see whether these common features were conserved in the structure of ImI. The fact that ImI is so closely related to EpI, which antagonizes $\alpha_3\beta_2$ or $\alpha_3\beta_4$ neuronal nAChRs, suggests that structural differences may account for their different yet related receptor specificities.

## Results

**Peptide Synthesis.** ImI was obtained in approximately 30% yield using a nonselective Boc chemistry synthesis strategy.[28] Formation of the disulfide bonds was achieved by air oxidation in a 50% 2-propanol/0.1 M ammonium bicarbonate (pH 8.0) buffer, which gave one major (>90%) peak. This was found to be a superior oxidation medium to aqueous ammonium bicarbonate buffer. Biological activity of synthetic ImI was confirmed in a nicotinic acetylcholine receptor assay,[29] and the NMR data (below) showed the disulfide connectivity to be identical to native.[3]

**NMR Data.** ImI gave good quality NMR spectra in aqueous solution over the pH range 3.1−6.1 and temperature range 280−295 K. Figure 2 shows the spin-system assignments in the TOCSY spectrum and their sequential connectivity in the Hα−HN region of the NOESY spectrum at 280 K. Peaks for Arg7 and Arg11 are slightly broadened; however, no other spectral inhomogenities are observed, indicating the presence of a predominant single conformation in solution, with possible conformational flexibility associated with the two long Arg side chains. $^1H$ and $^{13}C$ chemical shift assignments are provided as Supporting Information. In addition to the NMR data recorded in aqueous solution, a series of spectra was recorded in mixed aqueous/organic solvents to probe the role of solvent environment on structural stability. Solvent mixtures examined included 20% acetonitrile/water and 50% trifluoroethanol/water.

NOE connectivities, $D_2O$ exchange, and HN−Hα coupling data are summarized in the top panel of Figure 3. Eight out of 10 amide protons are observable in 1D spectra after dissolution in $D_2O$. Six of these amides are

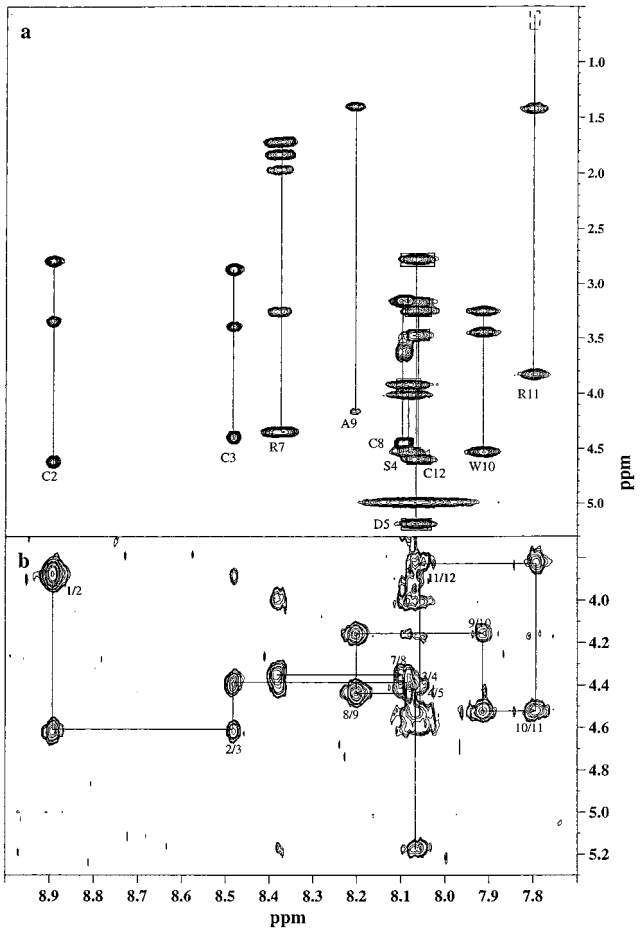


**Figure 2.** Regions of the 80-ms TOCSY spectrum (top) and 200-ms NOESY spectrum of ImI in 90% $H_2O$/10%$D_2O$ at 280 K, pH 3.1. Spin-systems are shown in the TOCSY spectrum and the sequential connectivities in the αH−NH region of the NOESY spectrum. The one-letter code for amino acids combined with the residue number is used in the labeling of these spectra.

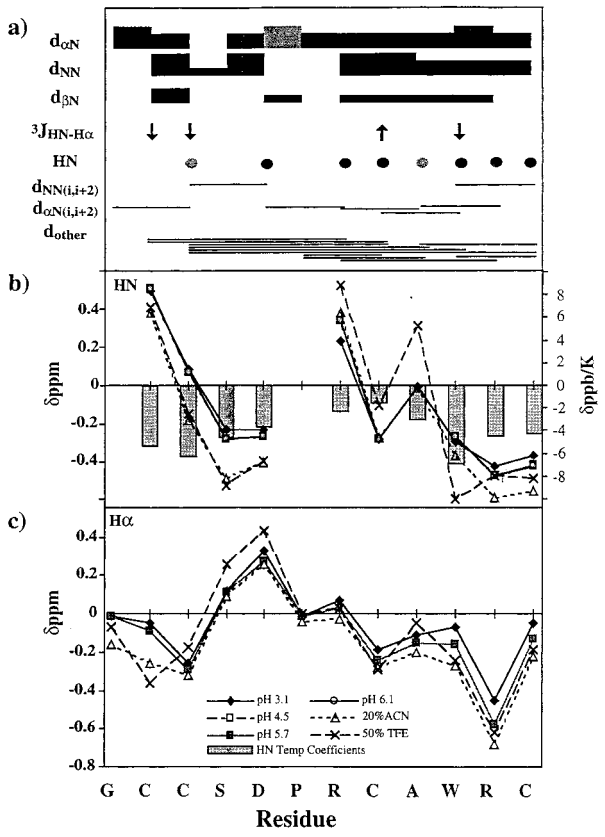


**Figure 3.** (a) Summary of the sequential and medium to long range NOE information, $^3J_{HN-H\alpha}$ coupling constants, and slow-exchange HN data. The top three lines give the sequential NOE data, with the height of the bars indicating the relative NOE strength (strong, medium, or weak). Gray-shaded NOEs are shown for the sequential NOEs from Asp5 to the δ protons of Pro6. ↑ and ↓ symbols represent $^3J_{NH-\alpha H}$ coupling constants of ≥8.5 and ≤5.0 Hz, respectively. Filled circles indicate slow-exchange amide protons, gray circles represent a HN signal was seen in 1D spectra for at least 10 min, and black circles represent protons present for more than 2 h after dissolution in 100% $D_2O$ at 280 K. For the $\mathbf{d_{other}}$ line of the NOE summary diagram, solid lines represent one or more NOEs between any protons of the starting and ending point residues of that particular line. These data are presented in this way to give an indication of the number of medium to long range NOEs observed. (b,c) Deviation from random coil chemical shift values for ImI HN (b) and Hα (c) protons. Deviations were calculated by subtracting random coil values[59] from the chemical shifts. Corrections for residues preceding Pro were applied. The gray bars in panel b show the deviation from random coil NH temperature coefficients for ImI, with values corresponding to the right-hand axis. NH chemical shifts were obtained from TOCSY spectra at 280, 285, 290, and 295 K. Lines of best fit were calculated, and the slope of these lines were used as the temperature coefficients. Random coil temperature coefficients[30] were subtracted from the experimental data and the resultant deviations plotted, with a negative deviation indicating a solvent-protected amide proton.

present after 2 h, and four are still present after 12 h, which provides evidence for a solvent-protected or hydrogen-bonded backbone. No helical structure is indicated by the NOE patterns in Figure 3 as there are no repeated $H\alpha-HN_{(i-i+3)}$ or $H\alpha-HN_{(i-i+4)}$ NOEs, as would be expected for a $3_{10}$ or regular α helix. Both of these types of helix had been observed for other α-conotoxin structures. However, several $H\alpha_{(i-i+2)}$ NOEs indicate possible nested turns. A strong NOE is observed between the Hα−Hδ protons for Asp5−Pro6, indicative of a trans peptide bond. Further, the Cβ−Cδ $^{13}C$ chemical shift difference is 4.9 ppm, consistent with a *trans*-proline,[31] compared to an expected value of >10 ppm for a *cis*-proline.

Panels b and c of Figure 3 show HN chemical shift/temperature coefficients as well as deviations from random coil chemical shifts (commonly referred to as secondary shifts) for Hα and HN protons under different pH and solvent conditions. The temperature coefficients provide a measure of the degree of solvent protection that is complementary to slow-exchange data.[30] In general, negative deviations from random coil values of more than 3 ppb/K indicate a degree of solvent protection. The secondary shifts provide a measure of changes in local structure.

It appears that ImI has a well-defined, stable backbone in solution, as the HN protons have secondary shifts which are resistant to changes in pH (pH 3.1−6.1) and have large negative deviations from random coil HN temperature coefficients. The effects of 20% ACN or 50% TFE on chemical shifts are only minor: HN secondary shifts for residues in the first loop (Cys2−Asp5) are all more negative by approximately 0.2 ppm on titration with organic solvents; a combination of upfield and downfield shifts is observed for the C-

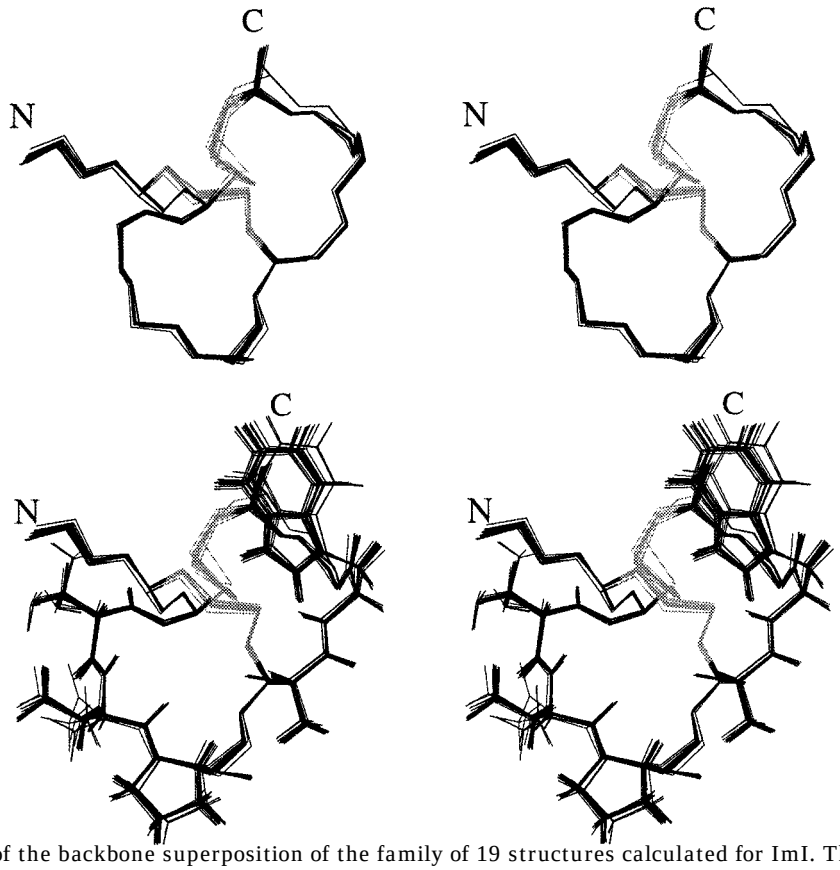


**Figure 4.** Stereoview of the backbone superposition of the family of 19 structures calculated for ImI. The disulfides are shaded in gray and the N- and C-termini labeled. The structures shown in the bottom half of the diagram are in an identical orientation to the top of the diagram and display the side chains of all residues excluding the disordered arginine side chains.

terminal part of the molecule. The Hα secondary shifts, which are more indicative of backbone structure, change only marginally with addition of 20% ACN and only slightly more with 50% TFE. Once again the first five residues are affected to a somewhat greater extent than the second half of the molecule. Overall, the solvent and pH data suggest that the solution conformation is not significantly affected by the solution environment. Further the HN−HN NOE pattern in 50% TFE was identical to that in the $H_2O$ spectra. Thus, it was not considered necessary to quantitatively determine structures under the different solution conditions, and all subsequent data reported here refer to aqueous solution.

One of the H$\beta$ protons of Cys8 is somewhat unusual in that it is broad and somewhat shifted downfield of the usual H$\beta$ chemical shift for Cys (3.67 ppm, compared to ∼3.30 ppm). It is interesting to note that upon addition of 50% TFE this resonance sharpens and shifts even further downfield to 4.12 ppm, close the Hα chemical shift. This pattern is also observed for EpI in aqueous solution and for PnIA and PnIB in 20−30% ACN (manuscript in preparation).

**Structural Data.** A total of 117 distance restraints (40 intraresidue, 44 sequential, 17 medium, and 16 long range) were obtained from 500- and 750-MHz data. Three $\phi$ angle restraints of $-65 \pm 30°$ (Cys2, Cys3, and Trp10) and one $\phi$ angle restraint of $-120 \pm 40°$ (Cys8) were obtained from 1D and DQF-COSY spectra. Two $\chi_1$ angle restraints of $180 \pm 30°$ (Cys2 and Cys3) and one $\chi_1$ angle restraint of $60 \pm 30°$ (Trp10) were obtained from a combination of ECOSY and NOESY spectra. The NOE and dihedral restraints were combined with the backbone Hα chemical shift data and used in a torsion angle dynamics calculation using XPLOR[32,33] to determine a family of 3D structures. This protocol produced similar structures to one which did not involve torsion angle dynamics or chemical shift refinement,[20] except that better convergence of the structures was obtained using the new protocol.

The 19 lowest energy structures from 50 were chosen as the final ensemble, with backbone pairwise rmsd of 0.34 Å, 1.40 Å for all heavy atoms, no NOE violations >0.2 Å, and fewer than three NOE violations >0.1 Å. Angular order parameters, which provide a measure of the precision of the calculated structures, are available as Supporting Information. To summarize, $S$ values >0.99 were obtained for all residues except Cys12 ($S$ = 0.84).

The high quality of the structures is evident from the superpositions shown in Figure 4, where even side chain orientations are well-defined for most residues. Relevant geometric and energetic statistics, as well as Ramachandran plot statistics, are given in Table 1. Structures calculated without the chemical shift refinement step were slightly less precise, with the 20 lowest energy structures having a backbone pairwise rmsd of 0.78 Å; however, the fold and disposition of the side chains were identical.

Hydrogen bonds were not used as restraints in the structure calculations; however, inspection of the resultant structures suggested main-chain hydrogen bonds between the carbonyl oxygen of Cys2 and the amide proton of Asp5, as well as between the carbonyl oxygen of Asp5 and the amide proton of Cys8 in all 19 structures, accounting for the slow-exchange and low-temperature coefficients for the amide protons of Asp5

**Table 1.** Geometric and Energetic Statistics for the 19 Lowest Energy Structures of ImI

| | |
|---|---|
| rmsd from Experimental Restraints | |
| interproton distances (Å) | 0.014 ± 0.002 |
| dihedral angles (deg) | 0.016 ± 0.02 |
| rmsd from Idealized Geometry | |
| bonds (Å) | 0.008 ± 0.0004 |
| angles (deg) | 2.42 ± 0.04 |
| impropers (deg) | 0.17 ± 0.02 |
| Energies (kcal mol$^{-1}$) | |
| $E_{NOE}$ | 0.62 ± 0.19 |
| $E_{cdih}$ | 0.0002 ± 0.001 |
| $E_{L-J}$ | −45.1 ± 2.2 |
| $E_{bond} + E_{angle} + E_{improper}$ | 29.5 ± 1.0 |
| Ramachandran Plot Regions | |
| % in favored | 59 |
| % in additional allowed | 37 |
| % in generously allowed | 4 |
| % in disallowed | 0 |

and Cys8. The proximity of the Trp aromatic ring to the Cys2−Cys8 disulfide bond appears to account for the downfield-shifted H$\beta$ peak observed for Cys8. In the calculated structures the HB2 proton of Cys8 is in the plane of the Trp ring and would be expected to be downfield-shifted.

The consensus elements of secondary structure in ImI consist of two type I $\beta$ turns between residues 1−4 and 2−5 and three type IV $\beta$ turns between residues 5−8, 6−9, and 9−12. Each turn type occurs in at least 16/19 structures. While hydrogen bonds were not formally identified for the last three of these turns, the observed slow-exchange behavior of residues 8, 9, and 12 is consistent with the proposed turn assignments.

The global fold of ImI is unusually compact for a peptide of this size and is best described as a series of adjacent and/or overlapping turns which are stabilized by two disulfide bonds. These disulfide bonds form the core of the molecule and are remarkably shielded from solvent. The Cys2−Cys8 disulfide bond is in a right-hand hook conformation for 18/19 structures, with the other one as left-handed spiral. The Cys3−Cys12 disulfide bond adopts left-handed conformations in all of the structures. The very tight packing of ImI is consistent with our observations that the solvent environment and pH have little influence on the structure.

## Discussion

The structure of ImI is well-defined in aqueous solution, with a total backbone pairwise rmsd of 0.34 Å. The structure appears stable under a range of pH and solvent conditions as only very small changes in chemical shifts were detected under different conditions. The side chains are very well-defined, with the exception of Arg7 and Arg11. The molecule adopts a cylindrical, or barrel shape, with Arg11 sticking out of one end of the barrel. The length of the barrel (excluding the protruding Arg) is ∼12 Å, and its diameter is 8−9 Å.

The molecule is held together in this tight conformation by two disulfide bridges, which fill the core of the molecule. The Trp10 side chain is oriented close to the "top" of the disulfide core. The disulfide bond Cys2−Cys12 has a right-handed conformation which is the less common handedness of disulfide bonds. All previously published α-conotoxin structures have had a left-handed conformation for the "first" disulfide (i.e. between the first and third cysteines), and only GI has had a right-handed conformation for the second disulfide bond. However, the loop sizes of ImI are different from those of any previously published structure, and the somewhat more strained structure may force the right-handedness. It is interesting that the only other right-handed disulfide was observed for GI, which also has smaller loop sizes between the cysteine residues.

Three of the four residues required for binding of the $\alpha_7$ neuronal nAChR (Asp5, Pro6, and Arg7)[34] are situated at the N-terminal end of the molecule and are clustered together near the bottom of the barrel and toward one side of it (Figure 5). Although the other

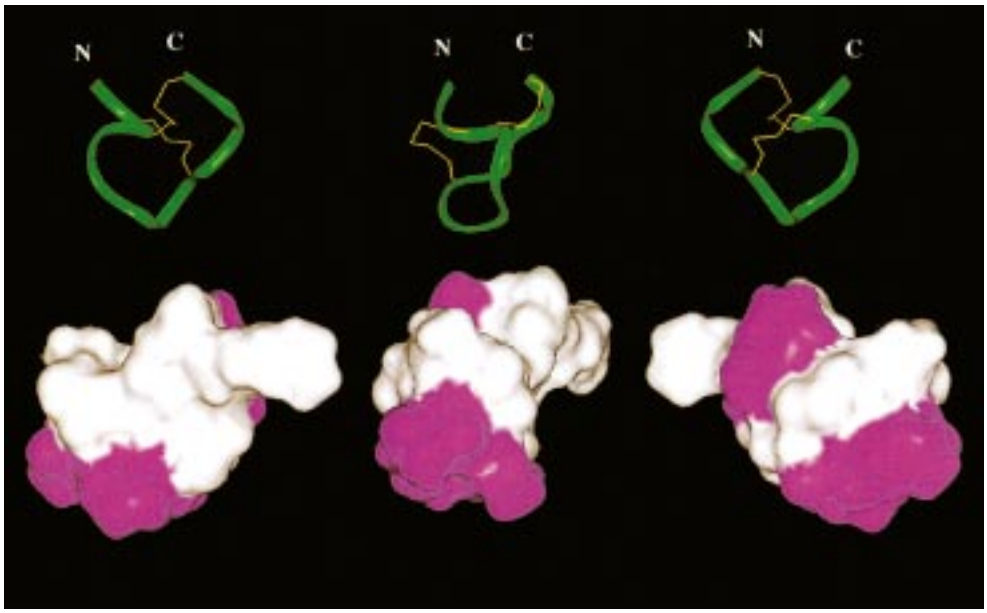


**Figure 5.** (Top) Ribbon diagrams of the lowest energy structure of ImI shown in three orientations rotated by 90° around the *y*-axis, to demonstrate the dimensions of the molecule. The disulfide bonds are shown in yellow, and the N- and C-termini are labeled. (Bottom) Connolly surfaces of ImI for the orientations shown in the top panel, calculated with a probe radius of 1.4 Å using the program Insight95. The residues shown in pink correspond to Asp5, Pro6, Arg7, and Trp10 which have been shown to be important for binding to the α7 neuronal nAChR.[34] The remainder of the molecule is shown in white.

essential binding residue, Trp10, is located near the C-terminus, it is on one side of the barrel and quite close to the other three binding residues. We thus suggest that the surface patch defined by these four residues forms the binding surface of the molecule. This is strongly reinforced by the observation that those residues which have been shown not to affect binding (Gly1, Ser4, Ala9, and Arg11)[34] are all located on the opposite side of the barrel to the binding surface (Figure 5). This further suggests that despite the very small size and compact structure of ImI, it interacts only using one face of the molecule.

It is interesting to note that the first eight residues of ImI are identical to those of the recently isolated EpI,[4] which has a much larger second loop containing seven, rather than three, residues. There is very little homology between the second loop of these two molecules, though both contain aromatic residues. EpI is thought to bind to $\alpha_3\beta_2$, $\alpha_3\beta_4$, or both types of neuronal nAChRs of rats but does not appear to bind to the rat $\alpha_7$ neuronal nAChR. Because of some shared common features and some significant differences, it was of interest to compare the structures of ImI and EpI. This comparison was also extended to GI as a representative of the 3/5 family of conotoxins.

**Comparison with Structures of EpI and GI.** As noted in the Introduction, ImI is the only known member of the 4/3 family of α-conotoxins. It is of interest to compare the ImI structures determined here with those of EpI,[27] a 4/7 family member, and GI,[20,24] a 3/5 family member. Backbone superpositions for the solution structure of ImI with the X-ray structure of EpI and NMR structure of GI are shown in Figure 6.

The first loops of ImI and EpI have an almost identical conformation. The backbone rmsd over these residues is 0.98 Å. By contrast, the fit over loop 2 is, not unexpectedly, much poorer, suggesting that the specificity variation between these two molecules probably arises from differences in loop 2. It is clear that EpI has a much bulkier loop 2, due to the extra four residues, which stabilize a section of regular α helix between residues 6−11. Further, EpI has a negative charge in this loop, whereas ImI has a positive charge.

It will be of great interest to determine if the selectivity between these two molecules for two different types of neuronal nAChR arises from EpI simply not being able to fit into the $\alpha_7$ subunit binding site, due to its greater size, and ImI not binding to the $\alpha_3\beta_2$ or $\alpha_3\beta_4$ nAChRs of mice, due to a small clash from the second loop. Recent data suggests that ImI may be able to bind to $\alpha_3\beta_4$ nAChRs from bovine chromaffin cells,[29] which could be explained by only minor differences in the receptor sequences. Mutating the Arg11 to a shorter neutral or negatively charged residue like Ser or Glu could possibly turn ImI into an $\alpha_3\beta_2$ or $\alpha_3\beta_4$ antagonist. Some residues of the α7 subunit which are involved in ImI binding have been identified (Trp55, Ser59, and Thr77),[35] and hence similar residues on the $\alpha_3\beta_2$ or $\alpha_3\beta_4$ nAChRs may help to model the structure of the whole extracellular domain of the nAChRs.

ImI could not easily be superimposed with GI, as is clear from the lower panel of Figure 6. Various superimposition modes were tried, and none highlighted any obvious similarities. The following rmsd values were obtained between ImI and the NMR structure of GI: all Cys heavy atoms superimposed to 2.7 Å, Cys C$\beta$ and S$\gamma$s superimposed to 1.55 Å; the backbone atoms of ImI 2, 3, 6, 8, 10, and 12 had an rmsd of 2.7 Å with GI residues 2, 3, 5, 6, 11, and 13, an alignment based on the cysteines, the conserved loop 1 proline, and the two aromatic residues Trp10 (ImI) and Tyr11 (GI).


**Figure 6.** (Top) Backbone superposition for ImI with the X-ray structure of EpI,[27] EpIB—the second molecule in the asymmetric unit of EpI. There are two structures of EpI in the asymmetric unit, EpIA and EpIB, and EpIB was chosen as the "representative" molecule, as Arg7 is actually modeled rather than an alanine in EpIA. The backbone rmsd for residues 1−8 in ImI and EpIB is 1.02 Å. (Bottom) Backbone superposition for ImI with the high-resolution NMR structure of GI,[20] superimposed over the cysteine side chains as well as the conserved proline.

## Conclusions

The α-conotoxin ImI, isolated from the worm-hunting *C. imperialis*,[3] differs from all other conotoxins in its high selectivity for the neuronal $\alpha_7$-containing nAChR. Neuronal nAChRs have been implicated in the treatment of several disease states as high doses of nicotine are beneficial to sufferers from cognitive and attention deficits, Parkinson's disease, Tourette's syndrome, ulcerative colitis, and schizophrenia.[16] Further, it is believed that $\alpha_7$-containing nAChRs have an active role in neuronal growth, development, and plasticity,[10,13] as well as neuronal signal modulation.[11] Structural information from the toxin ImI defines the binding surface to the receptor and combined with data available for

related, larger α-conotoxins such as EpI, PnIA, and PnIB will help with modeling the whole extracellular domain of this large receptor family.

It is very important to understand the structural origin for the different selectivities of toxins that target the nAChR, so that highly selective antagonists and agonists for the various receptor subtypes can be developed. The therapeutic potentials of nicotine cannot be fully realized unless the harmful side effects associated with nonspecific interactions can be eliminated.[16] The structure of ImI reported here brings us a step closer to designing molecules which may distinguish between the different neuronal nAChR subtypes.

## Experimental Section

**Synthesis.** ImI was assembled on *p*-MBHA resin (Peninsula Labs) using an in situ neutralization protocol for Boc chemistry.[28] Boc-Ala, Asp(OcHxl), Arg(Tos), Cys(MeBzl), Gly, Pro, and Ser(Bzl) were from the Peptide Institute, Osaka, Japan, Boc-Trp(CHO) was from Auspep, Melbourne, Australia. All reagents were of synthesis or HPLC grade. The Trp formyl group was removed with 2 × 30-min treatments of 1.5 g of ethanolamine, 1.25 mL of $H_2O$, and 23.75 mL of DMF, prior to cleavage from resin. The assembled peptide was cleaved from the resin using liquid hydrogen fluoride (HF):*p*-cresol: p-thiocresol (18:1:1) at 0−2 °C for 2 h. The crude peptide was purified on a Vydac $C_{18}$ column, with a gradient of 0−40% B over 60 min (A = 0.1% trifluoroacetic acid (TFA) in $H_2O$, B = 0.09% TFA in 90% acetonitrile/$H_2O$). Pure toxin, assessed by analytical $C_{18}$ HPLC and electrospray mass spectrometry ($MH^+$ = 1351.5, calcd = 1352.6) was obtained in ∼30% yield.

**NMR.** The NMR samples were made up at ∼3 mM peptide in $D_2O$ or 90% $H_2O$/10% D2O at pH 3.1 (uncorrected meter reading), as well as 10 and 20% $CD_3CN/H_2O$ and 50% TFE/$H_2O$. TOCSY,[36] NOESY,[37,38] DQF-COSY,[39] and HMQC[40] spectra were acquired on either a Bruker ARX 500-MHz or an AVANCE 750-MHz spectrometer with a shielded gradient unit. Spectra were routinely acquired at 280 K and referenced to an internal DSS standard after acquisition of all other experiments. The temperature was maintained within ±0.1 K using a BT V2000 control unit and a Bruker BCU refrigeration unit. NOESY spectra were acquired with 50-, 200-, 300-, and 500-ms mixing times and TOCSY spectra with an 80-ms mixing time. Water suppression in TOCSY and NOESY spectra was achieved using a modified watergate[41] sequence, consisting of two sine-shaped gradient pulses on either side of a binomial 3−9−19 pulse of 10-kHz field strength. Water suppression for DQF-COSY spectra and all $D_2O$ spectra was achieved by use of low-power irradiation at the water resonance during the relaxation delay (1.8 s). The relaxation delay for the partial organic solvent systems was increased to 2.5 s for all spectra. All spectra were obtained in phase-sensitive mode using time proportional phase incrementation.[42] Spectra were acquired with 4096 data points in $F_2$ and 400−512 in $F_1$ and multiplied with squared sine bell window functions shifted by 90°. The data were zero-filled to give matrix sizes of 2048 × 2048 real data points.

Information on slowly exchanging amide protons was obtained by acquisition of 1D and TOCSY spectra immediately upon dissolution of a fully protonated peptide in $D_2O$. Additional information for the backbone HN resonances was acquired from TOCSY spectra in 90% $H_2O$/10% $D_2O$ recorded at pH 3.5, 3.9, 4.5, 5.1, 5.7, and 6.1, as well as at 285, 290, and 295 K to determine HN temperature coefficients. $^3J_{HN-C\alpha H}$ coupling constants were measured from the 1D spectrum where possible, or from the DQF-COSY for overlapped signals. Spectra were processed on a Silicon Graphics Indigo Workstation using UXNMR or XWINNMR (Bruker).

**Structure Calculations.** NOE restraints were obtained from the 200- and 300-ms NOESY spectra, and were classed as either strong (1.8−2.7 Å), medium (1.8−3.5 Å), or weak (1.8−5.0 Å).[43,44] Pseudo-atom corrections of 1.5 Å for methyl, 1.0 Å for methylene, and 2.0 Å for tyrosine ring protons were added.[45] Backbone dihedral restraints of $-60 \pm 30°$ were applied for $^3J_{HNC\alpha H} < 5$ Hz and $-120 \pm 40°$ for $^3J_{HNC\alpha H} > 8.5$ Hz.

NOE distances and dihedral restraints for the major conformations of each of the isomers were used in the program XPLOR (version 3.85)[46,47] to calculate a family of three-dimensional structures. All calculations were carried out on sequences with amidated C-termini, as restraints to these were obtained.

Molecular dynamics (MD) calculations involved two stages. First 50 starting structures with random $\phi-\psi$ angles were generated using the standard XPLOR geometric force field. High-temperature torsion angle dynamics[32,48] was carried out for 15 ps with the structures coupled to a 50 000 K temperature bath, with NOE and dihedral restraint force constants of 150 and 100 kcal/mol and the disulfide bonds represented by a pseudo-NOE of 2.02 Å with no force constant at this stage. Proline rings were kept planar during this stage. The dihedral restraints were then increased to 200 kcal and a force constant of 1000 kcal applied to the disulfide bond NOE, and 15 ps of cooling in 500 K steps was carried out. The cooled structures were minimized, with the disulfides covalently joined and $^1H$ Hα chemical shift restraints[33] turned on with a 7.5-kcal force constant. A further set of structures was also calculated without the Hα chemical shifts for comparison. The structures thus generated were minimized using the conjugate gradient Powell algorithm[49] in the CHARMm force field of XPLOR.[50]

The coordinates of ImI have been deposited with the Brookhaven Protein Data Bank (ID code 1cnl).

**Structure Analysis.** Consensus sequences were calculated using Promotif-NMR.[51] Structures were further analyzed using Procheck-NMR[52] and visualized using the program Insight95 (Biosym). Hydrogen bonds were calculated with the program HBPLUS.[53]

**Acknowledgment.** D.J.C. is an Australian Research Council Senior Fellow. J.G. was supported by an Australian Postgraduate Award and Centre for Drug Design and Development Postgraduate Scholarship. We are grateful to Bruce Livett, John Down, and Natalie Broxton for collaborations on mammalian nAChR pharmacology.

**Supporting Information Available:** $^1H$ and $^{13}C$ chemical shift assignments for ImI and a table of angular order parameters for the 19 lowest energy structures calculated for ImI. This material is available free of charge via the Internet at http://pubs.acs.org.

## References

(1) Olivera, B. M.; Rivier, J.; Clark, C.; Ramilo, C. A.; Corpuz, G. P.; Abogadie, F. C.; Mena, E. E.; Woodward, S. R.; Hillyard, D. R.; Cruz, L. J. Diversity of *Conus* neuropeptides. *Science* **1990**, *249*, 248−263.

(2) Myers, R. A.; Cruz, L. J.; Rivier, J. E.; Olivera, B. M. *Conus* peptides as chemical probes for receptors and ion channels. *Chem. Rev.* **1993**, *93*, 1923−1936.

(3) McIntosh, J. M.; Yoshikami, D.; Mahe, E.; Nielsen, D. B.; Rivier, J. E.; Gray, W. R.; Olivera, B. M. A nicotinic acetylcholine receptor ligand of unique specificity, α-Conotoxin ImI. *J. Biol. Chem.* **1994**, *269*, 16733−16739.

(4) Loughnan, M.; Bond, T.; Atkins, A.; Cuevas, J.; Adams, D. J.; Broxton, N.; Livett, B.; Down, J.; Jones, A.; Alewood, P. F.; Lewis, R. J. α-Conotoxin EpI: a novel sulfated peptide from *Conus episcopatus* which selectively targets neuronal nicotinic acetylcholine receptors. *J. Biol. Chem.* **1998**, *273*, 15667−15674.

(5) Fainzilber, M.; Hasson, A.; Oren, R.; Burlingame, A. L.; Gordon, D.; Spira, M. E.; Zlotkin, E. New mollusc-specific α-conotoxins block Aplysia neuronal acetylcholine receptors. *Biochemistry* **1994**, *33*, 9523−9529.

(6) Cartier, G. E.; Yoshikami, D.; Gray, W. R.; Luo, S.; Olivera, B. M.; McIntosh, J. M. A new α-conotoxin which targets α3β2 nicotinic acetylcholine receptors. *J. Biol. Chem.* **1996**, *271*, 7522−7528.

(7) Myers, R. A.; Zafaralla, G. C.; Gray, W. R.; Abbott, J.; Cruz, L. J.; Olivera, B. M. α-Conotoxins, small peptide probes of nicotinic acetylcholine receptors. *Biochemistry* **1991**, *30*, 9370−9377.

(8) Aprison, M. H.; Galvez-Ruano, E.; Lipkowitz, K. B. Comparison of binding mechanisms at cholinergic, serotonergic, glycinergic and GABAergic receptors. *J. Neurosci. Res.* **1996**, *43*, 127−136.
(9) Galzi, J.; Revah, F.; Bessis, A.; Changeux, J. Functional architecture of the nicotinic acetylcholine receptor: From electric organ to brain. *Annu. Rev. Pharmacol. Toxicol.* **1991**, *31*, 37−72.
(10) Pugh, P. C.; Berg, D. K. Neuronal acetylcholine receptors that bind α-bungarotoxin mediate neurite retraction in a calcium-dependent manner. *J. Neurosci.* **1994**, *14*, 889−896.
(11) McGehee, D. S.; Heath, M. J. S.; Gelber, S.; Devay, P.; Role, L. W. Nicotine enhancement of fast excitatory synaptic transmission in CNS by presynaptic receptors. *Science* **1995**, *269*, 1692−1696.
(12) Johnson, D. S.; Martinez, J.; Elgoyhen, A. B.; Heinemann, S. F.; McIntosh, J. M. α-Conotoxin ImI exhibits subtype-specific nicotinic acetylcholine receptor blockade: Preferential inhibition of homomeric α7 and α9 receptors. *Mol. Pharmacol.* **1995**, *48*, 194−199.
(13) Role, L. W.; Berg, D. K. Nicotinic receptors in the development and modulation of CNS synapses. *Neuron* **1996**, *16*, 1077−1085.
(14) Freedman, R.; Byerley, W. Linkage of a neurophysiological deficit in schizophrenia to a chromosome 15 locus. *Proc. Natl. Acad. Sci. U.S.A.* **1997**, *94*, 587−592.
(15) Chan, J.; Quik, M. A role for the nicotinic α-bungarotoxin receptor in neurite outgrowth in PC12 cells. *Neuroscience* **1993**, *56*, 441−451.
(16) Holladay, M. W.; Dart, M. J.; Lynch, J. K. Neuronal nicotinic acetylcholine receptors as targets for drug discovery. *J. Med. Chem.* **1997**, *40*, 4169−4194.
(17) Unwin, N. Nicotinic acetylcholine receptor at 9 Å resolution. *J. Mol. Biol.* **1993**, *229*, 1101−1124.
(18) Unwin, N. Acetylcholine receptor channel imaged in the open state. *Nature* **1995**, *373*, 37−43.
(19) Pardi, A.; Galdes, A.; Florance, J.; Maniconte, D. Solution structures of α-Conotoxin G1 determined by two-dimensional NMR spectroscopy. *Biochemistry* **1989**, *28*, 5494−5501.
(20) Gehrmann, J.; Alewood, P. F.; Craik, D. J. Structure determination of the three disulfide bond isomers of α-conotoxin GI: a model for the role of disulfide bonds in structural stability. *J. Mol. Biol.* **1998**, *278*, 401−415.
(21) Gouda, H.; Yemazaki, K.-i.; Hasegawa, J.; Kobayashi, Y.; Nishiuchi, Y.; Sakakibara, S.; Hirono, S. Solution structure of α-conotoxin MI determined by $^1H$ NMR spectroscopy and molecular dynamics simulation with the explicit solvent water. *Biochim. Biophys. Acta* **1997**, *1343*, 327−334.
(22) Shon, K.-J.; Koerber, S. C.; Rivier, J. E.; Olivera, B. M.; McIntosh, J. M. Three-dimensional solution structure of α-Conotoxin MII, an α3β2 neuronal nicotinic acetylcholine receptor-targeted ligand. *Biochemistry* **1997**, *36*, 15693−15700.
(23) Hill, J. M.; Oomen, C. J.; Miranda, L. P.; Bingham, J.-P.; Alewood, P. F.; Craik, D. J. Three-dimensional solution structure of α-conotoxin MII by NMR spectroscopy: Effects of solution environment on helicity. *Biochemistry* **1998**, *37*, 15621−15630.
(24) Guddat, L. W.; Martin, J. A.; Shan, L.; Edmundson, A. B.; Gray, W. R. Three-dimensional structure of the α-conotoxin GI at 1.2 Å resolution. *Biochemistry* **1996**, *35*, 11329−11335.
(25) Hu, S.-H.; Gehrmann, J.; Guddat, L. W.; Alewood, P. F.; Craik, D. J.; Martin, J. L. The 1.1 Å crystal structure of the neuronal acetylcholine receptor antagonist, α-conotoxin PnIA from *Conus pennaceus*. *Structure* **1996**, *4*, 417−423.
(26) Hu, S.-H.; Gehrmann, J.; Alewood, P. F.; Craik, D. J.; Martin, J. L. Crystal structure at 1.1 Å resolution of α-conotoxin PnIB: Comparison with α-conotoxins PnIA and GI. *Biochemistry* **1997**, *36*, 11323−11330.
(27) Hu, S.-H.; Loughnan, M.; Miller, R.; Weeks, C. M.; Blessing, R. H.; Alewood, P. F.; Lewis, R. J.; Martin, J. L. The 1.1 Å resolution crystal structure of [Tyr$^{15}$]-EpI, a novel α-conotoxin from *Conus episcopatus*, solved by direct methods. *Biochemisty* **1998**, *37*, 11425−11433.
(28) Schnölzer, M.; Alewood, P.; Jones, A.; Alewood, D.; Kent, S. B. H. In situ neutralization in Boc-chemistry solid-phase peptide synthesis. *Int. J. Pept. Protein Res.* **1992**, *40*, 180−193.
(29) Broxton, N. M.; Down, J. G.; Gehrmann, J.; Alewood, P. F.; Satchell, D. G.; Livett, B. G. Alpha-Conotoxin ImI inhibits the alpha-bungarotoxin-resistant nicotonic response in bovine adrenal chromaffin cells. *J. Neurochem.* **1999**, *72*, 1656−1662.
(30) Merutka, G.; Dyson, H. J.; Wright, P. E. 'Random Coil' 1H chemical shifts obtained as a function of temperature and trifluoroethanol concentration for the peptide series GGXGG. *J. Biomol. NMR* **1995**, *5*, 14−24.
(31) Wüthrich, K.; Tun-kyi, A.; Schwyzer, R. Manifestation in the $^{13}C$ NMR spectra of two different molecular conformations of a cyclic pentapeptide. *FEBS Lett.* **1972**, *25*, 104−108.
(32) Rice, L. M.; Brunger, A. T. Torsion angle dynamics: Reduced variable conformational sampling enhances crystallographic structure refinement. *Proteins: Struct., Funct., Genet.* **1994**, *19*, 277−290.
(33) Kuszewski, J.; Gronenborn, A.; Clore, M. The impact of direct refinement against $^{13}C$ alpha and $^{13}C$ beta chemical shifts on protein structure determination by NMR. *J. Magn. Reson. Series B* **1995**, *106*, 92−106.
(34) Quiram, P. A.; Sine, S. M. Structural elements in alpha-conotoxin ImI essential for binding to neuronal alpha7 receptors. *J. Biol. Chem.* **1998**, *273*, 11007−11011.
(35) Quiram, P. A.; Sine, S. M. Identification of residues in the neuronal α7 acetylcholine receptor that confer selectivity for conotoxin ImI. *J. Biol. Chem.* **1998**, *273*, 11001−11006.
(36) Bax, A.; Davis, D. G. MLEV-17-based two-dimensional homonuclear magnetization transfer spectroscopy. *J. Magn. Reson.* **1985**, *65*, 355−360.
(37) Jeener, J.; Meier, B. H.; Bachmann, P.; Ernst, R. R. Investigation of exchange processes by two-dimensional NMR spectroscopy. *J. Chem. Phys.* **1979**, *71*, 4546−4553.
(38) Kumar, A.; Ernst, R. R.; Wüthrich, K. A two-dimensional nuclear Overhauser enhancement (2D NOE) experiment for the elucidation of complete proton−proton cross-relaxation networks in biological macromolecules. *Biochem. Biophys. Res. Commun.* **1980**, *95*, 1−6.
(39) Rance, M.; Sorensen, O. W.; Bodenhausen, G.; Wagner, R.; Ernst, R. R.; Wüthrich, K. Improved spectral resolution in COSY $^1H$ NMR spectra of proteins via double quantum filtering. *Biochem. Biophys. Res. Commun.* **1983**, *27*, 157−162.
(40) Bax, A.; Griffey, R. H.; Hawkins, B. L. Correlation of proton and nitrogen-15 chemical shifts by multiple quantum NMR. *J. Magn. Reson.* **1983**, *55*, 301−315.
(41) Piotto, M.; Saudek, V.; Sklenar, V. Gradient-tailored excitation for single-quantum NMR spectroscopy of aqueous solutions. *J. Biomol. NMR* **1992**, *2*, 661−665.
(42) Marion, D.; Wüthrich, K. Application of phase sensitive two-dimensional correlated spectroscopy (COSY) for measurements of $^1H$-$^1H$ spin−spin coupling constants in proteins. *Biochem. Biophys. Res. Commun.* **1983**, *113*, 967−974.
(43) Williamson, M. P.; Havel, T. F.; Wüthrich, K. Solution conformation of proteinase inhibitor IIA from bull seminal plasma by $^1H$ nuclear magnetic resonance and distance geometry. *J. Mol. Biol.* **1985**, *182*, 295−315.
(44) Clore, G. M.; Nilges, M.; Sukuraman, D. K.; Brünger, A. T.; Karplus, M.; Gronenborn, A. M. The three-dimensional structure of α1-purothionin in solution: combined use of nuclear magnetic resonance, distance geometry and restrained molecular dynamics. *EMBO J.* **1986**, *5*, 2729−2735.
(45) Wüthrich, K. *NMR of proteins and nucleic acids*; Wiley-Interscience: New York, 1986.
(46) Brünger, A. T. *XPLOR Version 3.85 Manual*; Yale University: New Haven, CT, 1997.
(47) Brünger, A. T.; Clore, G. M.; Gronenborn, A. M.; Karplus, M. Three-dimensional structure of proteins determined by molecular dynamics with interproton distance restraints: application to crambin. *Proc. Natl. Acad. Sci. U.S.A.* **1986**, *83*, 3801−3805.
(48) Stein, E. G.; Rice, L. M.; Brunger, A. T. Torsion angle molecular dynamics as a new efficient tool for NMR structure calculation. *J. Magn. Reson.* **1997**, *124*, 154−164.
(49) Clore, G. M.; Brünger, A. T.; Gronenborn, A. M.; Karplus, M. Application of molecular dynamics with interproton distance restraints to three-dimensional protein structure determination. A model study of crambin. *J. Mol. Biol.* **1986**, *191*, 523−551.
(50) Brooks, B. R.; Bruccoleri, R. E.; Olafson, B. D.; States, D. J.; Swaminathan, S.; Karplus, M. CHARMM: a program for macromolecular energy, minimization and dynamics calculations. *J. Comput. Chem.* **1983**, *4*, 187−217.
(51) Hutchinson, E. G.; Thornton, J. M. PROMOTIF − A program to identify and analyze structural motifs in proteins. *Protein Sci.* **1996**, *5*, 212−220.
(52) Laskowski, R. A.; MacArther, M. W.; Moss, D. S.; Thronton, J. M. PROCHECK: a program to check the stereochemical quality of protein structure coordinates. *J. Appl. Crystallogr.* **1993**, *26*, 283−291.
(53) McDonald, I. K.; Thornton, J. M. Satisfying hydrogen bonding potential in proteins. *J. Mol. Biol.* **1994**, *238*, 777−793.
(54) Martinez, J. S.; Olivera, B.; Gray, W. R.; Craig, A. G.; Groebe, D. R.; Abramson, S. N.; McIntosh, J. M. α-Conotoxin EI, A new nicotinic acetylcholine receptor antagonist with novel selectivity. *Biochemistry* **1995**, *34*, 14519−14526.
(55) Gray, W. R.; Luque, A.; Olivera, B. M.; Barrett, J.; Cruz, L. J. Peptide toxins from *Conus geographus* venom. *J. Biol. Chem.* **1981**, *256*, 4734−4740.
(56) McIntosh, M.; Cruz, L. J.; Hunkapiller, M. W.; Gray, W. R.; Olivera, B. M. Isolation and structure of a peptide toxin from the marine snail *Conus magus*. *Arch. Biochem. Biophys.* **1982**, *218*, 329−334.
(57) Zafaralla, G. C.; Ramilo, C.; Gray, W. R.; Karlstrom, R.; Olivera, B. M.; Cruz, L. J. Phylogenetic specificity of cholinergic ligands: α-Conotoxin SI. *Biochemistry* **1988**, *27*, 7102−7105.

(58) Ramilo, C. A.; Zafaralla, G. C.; Nadasdi, L.; Hammerland, L. G.; Yoshikami, D.; Gray, W. R.; Kristipati, R.; Ramachandran, J.; Miljanich, G.; Olivera, B. M.; Cruz, L. J. Novel α- and *ω*-Conotoxins from *Conus striatus* venom. *Biochemistry* **1992**, *31*, 9919−9926.

(59) Wishart, D. S.; Bigam, C. G.; Horm, A.; Hodges, R. S.; Sykes, B. D. $^{1}$H, $^{13}$C and $^{15}$N random coil NMR chemical shifts of the common amino acids. I. Investigations of nearest-neighbor effects. *J. Biomol. NMR* **1995**, *5*, 67−81.

JM990114P